Simulation and Optimization of NO_x Absorption System in Nitric Acid Manufacture

N. J. Suchak and J. B. Joshi
Dept. of Chemical Technology, University of Bombay, Matunga, Bombay 400 019, India

A mathematical model has been developed for the prediction of the optimum design of packed and plate columns for the manufacture of nitric acid. The effects of inlet NO_x composition, extent of oxidation and extent of absorption in each stage, temperature, and pressure have been included in the model. The optimization of the preoxidizer and the condenser has also been discussed.

Introduction

Absorption of NO_x is an important step in the manufacture of nitric acid. Absorption of NO_x gas is probably the most complex when compared with other absorption operations. This is for several reasons. First, the NO_x gas is a mixture of several components consisting of NO, NO_2, N_2O_3, N_2O_4, and so on. The absorption of NO_x gas in water results into two oxyacids, nitric acid, and nitrous acid. Secondly, several reversible and irreversible reactions occur in both gas and liquid phases. Thirdly, simultaneous absorption of many gases occurs followed by chemical reaction. Also, simultaneous desorption of many gases occurs preceded by chemical reaction. For example, the absorption of NO_2, N_2O_3, and N_2O_4 is accompanied by chemical reaction whereas the desorption of NO, NO_2, and HNO_2 is preceded by chemical reaction. Finally, heterogeneous equilibria prevail between gas-phase and liquid-phase components. Sherwood et al. (1975) and Joshi et al. (1985) have reviewed these aspects of NO_x absorption.

For the process design of NO_x absorption towers, it is necessary to understand the combined effects of several equilibria, including the rates of mass-transfer and chemical reaction. Further, substantial heat effects are associated with NO_x absorption; therefore, temperature variations need to be taken into account in the process design. There have been outstanding attempts in this direction. For instance, Koval and Peters (1960), Andrew and Hanson (1961), Koukolik and Marek (1968), Carleton and Valentin (1968), Hoftizer and Kwanten (1972), Makhotkin and Shamsutdinov (1976), Holma and Sohlo (1979), Emig et al. (1979), Counce and Perona (1979, 1980, 1983), Joshi et al. (1985), Miller (1987), and Wiegand et al. (1990) have reported various aspects of the process design of packed columns, plate columns, and packed bubble columns used for the manufacture of nitric acid. These attempts will be strengthened if the following important features are included in the process design.

(1) The rates of absorption of NO_2, N_2O_3, and N_2O_4 in nitric acid are different from those in water. The rates decrease with an increase in the concentration of nitric acid.

(2) It is known that for a given set of partial pressures of NO, NO_2, and N_2O_4, there exists a certain limiting concentration of nitric acid beyond which no absorption of N_2O_4 and NO_2 occurs (Carberry, 1958). This heterogeneous equilibrium substantially reduces (even three to four times) the rates of absorption of NO_2, N_2O_3, and N_2O_4, and the extent of reduction increases as the nitric acid concentration approaches the equilibrium value.

(3) A substantial quantity of nitric acid is formed in the gas phase, particularly at high temperatures and high partial pressure of NO_x. Therefore, HNO_3 formation needs to be included in the mathematical model.

(4) A detailed energy balance also needs to be incorporated in the model.

Table 1 summarizes the earlier work. Though the mathematical model of Suchak et al. considers all the above aspects, it was developed for a case of a four-stage absorption system. In the commercial process of nitric acid manufacture, a large number (exceeding 50) of absorption and oxidation stages are used. Under these conditions, there are several aspects which need to be considered for the reliable and optimal design. These are:

(1) For every mole of NO_x absorber, 1/3 mol is desorbed in the form of NO. Thus, the oxidation rates are linked with the absorption/desorption rates.

(2) The rate of absorption of NO_2 as such is negligible.

Correspondence concerning this article should be addressed to J. B. Joshi.
Current address of N. J. Suchak: Cannon Technologies, Inc., P. B. Box 1, New Kensington, PA 15068.

Table 1. Summary of Previous Work

	Dependence of $H\sqrt{kD}$ on HNO_3 Conc.	Role of Heterogeneous Equil. on Abs. Rate	Formation HNO_3 in Gas Phase	Mass Transfer of H_2O, HNO_3 and/or HNO_2 from/to Gas Phase from/to Liquid Phase	Complete Energy Balance
Emig et al. (1979)*	NC	NC	NC	NC	C
Holma & Sohlo (1979)**	NC	NC	NC	NC	C
Miller (1987)	C	NC	NC	NC	NC
Wiegand et al. (1990)*	C	NC	NC	NC	NC
Suchak et al. (1991)	C	C	C	C	C

*The mechanism of absorption with chemical reaction needs to be included in the overall rate equation.
**The plate efficiency needs to be calculated for the case of NO_x absorption.
C = Considered
NC = Not considered

However, in the presence of NO, NO_2 forms N_2O_3 and HNO_2 in the gas phase. The rate of N_2O_3 and HNO_2 absorption are very high. Thus, the presence of sufficient NO enhances the rate of absorption.

(3) The maximum permissible concentration of HNO_3 (l) decreases with an increase in mole fraction of NO. As the absorption continues, the mole fraction of NO increases because of the absorption of N_2O_4, N_2O_3, and HNO_3 (g). Therefore, the multistage operation is needed for getting the desired concentration of HNO_3 (l). Each stage consists of an absorption section and an oxidation section. For instance, in the case of a sieve plate column, the absorption occurs on the plate and the NO oxidation occurs in the empty space between the two plates. The plate spacing depends upon the extent of desired oxidation. The extent of absorption on a plate is also a variable.

(4) The effect of temperature is multifold. The rate of NO oxidation decreases whereas the rate of absorption increases with an increase in temperature. The conversion of NO_2 to N_2O_4 is favorable at lower temperature. Further, for a given NO_x composition in the gas space, the maximum permissible HNO_3 (l) concentration increases with a decrease in temperature.

(5) Total pressure is a very strong parameter. The rate of NO oxidation is proportional to the cube of pressure and the rates of absorption also increase with an increase in total pressure.

Since all the above parameters strongly interact, detailed understanding is needed for the selection of optimum design and operating parameters.

Mathematical Model

In the commercial nitric acid plant, the mixture of ammonia with air is passed over catalyst gauze at temperature and pressure in the range of 800–850°C and 0.3–2 MPa, respectively. The following is a major reaction:

$$4NH_3(g) + 5O_2(g) \longrightarrow 4NO(g) + 6H_2O(g) \qquad (1)$$

This is an exothermic oxidation reaction with a short residence time. Heat liberated is advantageously removed in heat recovery section to produce superheated steam, to preheat air, and in certain cases to preheat the tail gas. The gas stream leaving the heat recovery section is at a temperature above dew point (in a typical case 200°C) and is further cooled in a cooler/condenser before feeding it to an absorber.

The condensate is a weak nitric acid solution which is added up at an appropriate location in the absorption column.

Model for the cooler/condenser

In the cooler, the gas stream is directly contacted to weak aqueous solution of nitric acid. Mainly two types of coolers are employed: (i) spray type, where an aqueous weak acid solution is sprayed in the gas stream; (ii) bubble column type where the gas is bubbled through a pool of liquid. In both types of coolers, the weak nitric acid solution is directly brought in contact with the gas stream.

Condensers employed are generally large surface area heat exchangers. The hot gas from the heat recovery stream is passed over the cooler surface where part of water vapor condenses.

In cooler as well as condenser, during cooling, many chemical reactions and chemico-physical phenomena occur. They are: (i) oxidation of nitric oxide; (ii) formation of higher nitrogen oxides; (iii) condensation of water and oxy acids; (iv) absorption of nitrogen oxides.

In the process design of a nitric acid plant, the design of cooler/condenser is very important for obtaining the desired concentration of the product acid from the absorption section. Therefore, a mathematical model for the cooler/condenser is presented below.

Gas-phase reactions and equilibria

The gas entering the condenser consists of NO_x gases, nitrogen, oxygen, and water vapor. Nitric oxide undergoes irreversible oxidation with oxygen in the gas phase.

The oxidation reaction is expressed as:

$$2NO(g) + O_2(g) \xrightarrow{k_1} 2NO_2(g) \qquad (2)$$

Joshi et al. (1985) have reviewed the published literature on NO oxidation. It is believed that NO oxidation proceeds by dimerization of NO is followed by oxidation by oxygen to form N_2O_4. The oxidation reaction is second-order with respect to NO and first-order with respect to oxygen.

The gas phase consists of NO, NO_2, N_2O_3, and N_2O_4. In the

Table 2a. Gas-Phase Reactions

Eqs.	Equilibrium and Rate Constants	
1	$\log_{10} k_1 = 652.1/T - 4.747$	$(kN/m^2)^{-2}\cdot s^{-1}$
2	$\log_{10} K_2 = 2{,}993/T - 11.232$	$(kN/m^2)^{-1}$
3	$\log_{10} K_3 = 2{,}072/T - 9.2397$	$(kN/m^2)^{-1}$
4	$\log_{10} K_4 = 2{,}051.17/T - 8.7385$	$(kN/m^2)^{-1}$
5	$\log_{10} K_5 = 2{,}003.8/T - 10.763$	$(kN/m^2)^{-1}$

presence of water vapor (which is generally the case) oxyacids (HNO_2 and HNO_3) are also present in the gas phase. Complex equilibria prevail in the gas phase which can be described by the following equations:

$$2NO_2(g) \overset{K_2}{\rightleftharpoons} N_2O_4(g) \tag{3}$$

$$NO(g) + NO_2(g) \overset{K_3}{\rightleftharpoons} N_2O_3(g) \tag{4}$$

$$NO(g) + NO_2(g) + H_2O(g) \overset{K_4}{\rightleftharpoons} 2HNO_2(g) \tag{5}$$

$$3NO_2(g) + H_2O(g) \overset{K_5}{\rightleftharpoons} 2HNO_3(g) + NO(g) \tag{6}$$

The reaction rate constant k_1 and the gas-phase equilibria constants $K_2 \ldots K_5$ were reported by Joshi et al. (1985) and are presented in Table 2a.

The total number of moles in the gas per mole of inerts is obtained by adding ratios of all gaseous species to one mole of inerts:

$$Y_T = Y_{NO} + Y_{NO_2} + Y_{N_2O_4} + Y_{N_2O_3} + Y_{HNO_3} + Y_{HNO_2} + Y_{H_2O} + Y_{O_2} + 1.0 \tag{7}$$

where,

Table 2b. Heats of Reaction

Reactions	Std. Heat of Reaction (25°C) kcal × 10^{-3}
Reactions in Gas Phase	
$2NO_{(g)} + O_{2(g)} \longrightarrow 2NO_{2(g)}$	$\Delta H_1 = -13.64$ per kmol NO oxidized
$2NO_{2(g)} \longrightarrow N_2O_{4(g)}$	$\Delta H_3 = -13.69$ per kmol N_2O_4 formed
$NO_{(g)} + NO_{2(g)} \longrightarrow N_2O_{3(g)}$	$\Delta H_4 = -9.55$ per kmol N_2O_3 formed
$3NO_{2(g)} + H_2O_{(g)} \longrightarrow 2HNO_{3(g)} + NO_{(g)}$	$\Delta H_6 = -4.23$ per kmol HNO_3 formed
$NO_{(g)} + NO_{2(g)} + H_2O_{(g)} \longrightarrow 2HNO_{2(g)}$	$\Delta H_7 = -4.905$ per kmol HNO_2 formed
Reactions in the Liquid Phase	
per kmol NO_2 absorbed	$\Delta H_8 = -12.82$
per kmol N_2O_4 absorbed	$\Delta H_9 = -12.04$
per kmol N_2O_3 absorbed	$\Delta H_{10} = -9.55$
per kmol HNO_2 absorbed	$\Delta H_{13} = +5.71$
per kmol HNO_3 absorbed	$\Delta H_{11} = -9.36$
per kmol HNO_2 absorbed	$\Delta H_{12} = -9.9$

$$Y_{N_2O_4} = K_2 (Y_{NO_2})^2 P_T / Y_T \tag{8}$$

$$Y_{N_2O_3} = K_3 Y_{NO} Y_{NO_2} P_T / Y_T \tag{9}$$

$$Y_{HNO_2} = [K_4 Y_{NO} Y_{NO_2} Y_{H_2O} P_T / Y_T)^{1/2} \tag{10}$$

$$Y_{HNO_3} = \left(\frac{K_5 (Y_{NO_2})^3 Y_{H_2O}}{Y_{NO}} \frac{P_T}{Y_T} \right)^{1/2} \tag{11}$$

All the components of NO_x can be expressed in terms of:

(a) Total reactive nitrogen (Y_N*), mole of reactive nitrogen per mole of inerts:

$$Y_N^* = Y_{NO} + Y_{NO_2} + 2(Y_{N_2O_4}) + 2(Y_{N_2O_3}) + Y_{HNO_3} + Y_{HNO_2} \tag{12}$$

(b) while extent of oxidation at any instance is expressed in the form of Y_{NO}*, moles of divalent nitrogen per mole of inerts:

$$Y_{NO}^* = Y_{NO} + Y_{N_2O_3} + 0.5(Y_{HNO_2}) - 0.5(Y_{HNO_3}) \tag{13}$$

(c) Y_{H_2O}* is moles of water in the form of oxyacids and free water vapor per mole of inerts. It is expressed as:

$$Y_{H_2O}^* = Y_{H_2O} + 0.5(Y_{HNO_3}) + 0.5(Y_{HNO_2}) \tag{14}$$

Condensation and liquid-phase reactions

In the cooler/condenser, due to reduction in temperature, water vapor from the gas phase condenses with simultaneous absorption of nitrogen oxides thus further altering the equilibria. Nitrogen oxides when absorbed in an aqueous acid solution form nitrous and nitric acid. The following reactions occur in the liquid phase:

$$2NO_2(l) + H_2O(l) \longrightarrow HNO_3(l) + HNO_2(l) \tag{15}$$

$$N_2O_3(l) + H_2O(l) \longrightarrow 2HNO_2(l) \tag{16}$$

$$N_2O_4(l) + H_2O(l) \longrightarrow HNO_2(l) + HNO_3(l) \tag{17}$$

HNO_2 in the bulk of liquid phase is considered to decompose to form nitric acid:

$$3HNO_2(l) \longrightarrow HNO_3(l) + 2NO(l) + H_2O(l) \tag{18}$$

HNO_3 and H_2O are at their saturation concentrations in the gas phase. Vapor pressure of H_2O or HNO_3 over the aqueous nitric acid solution is a function of temperature and nitric acid concentration:

$$p_{H_2O} = f(T, \text{Conc}(HNO_3)) \tag{19}$$

$$p_{HNO_3} = f(T, \text{Conc}(HNO_3)) \tag{20}$$

Condensate concentration and heterogeneous equilibria

For a known composition of NO_x in the gas phase the maximum attainable concentration of nitric acid (in the liquid phase) is described by Carberry (1958):

$$K_6 = \frac{p_{NO}}{(p_{N_2O_4})^{3/2}} \quad (21)$$

Holma and Sohlo (1979) have given the following correlation for the equilibrium constant:

$$\log K_H = 30.086 - 0.0693T - (0.197 - 3.27 \times 10^{-4}\, T)\, W + 1.227 \log[(100 - W)/W^2] \quad (22a)$$

and for less than 5 percent by weight

$$\log K_H = 31.96 - 0.0693T - (3.27 \times 10^{-4}\, T - 0.4193)W \quad (22b)$$

where

$$K_H = K_2^{3/2} K_6 (101.33)^2 \quad (23)$$

and W is the maximum attainable HNO_3 concentration in weight percent. K_6 is given by Eq. 21.

Material balance over condenser/cooler

Here we make the following rational assumptions:

(1) All reacted nitrogen oxide entering the condenser is in the form of nitric oxide.

(2) Gases leaving the condenser are in equilibrium with condensate.

(3) Gases leaving the condenser are saturated with nitric acid and water vapor.

Water enters the condenser in the form of water vapor. Partly it condenses and partly it reacts to form nitric and nitrous acid in both liquid and gas phases. Equating the incoming and outgoing streams of condenser for H_2O^*:

$$G(Y_{H_2O^*,i}) = G(Y_{H_2O^*,C}) + L_C(1 + 0.5X_C) \quad (24)$$

As stated in the assumption, NO_x entering the condenser is in the form of nitric oxide while due to oxidation, gas-phase equilibrium, condensation, and absorption in the condenser, it is present in both gas and liquid phases. The balance for reactive nitrogen gives:

$$G(Y_{N^*,i}) = G(Y_{N^*,C}) + L_C(X_C) \quad (25)$$

Due to oxidation of nitric oxide to nitrogen dioxide, oxygen concentration in the gas phase reduces. The material balance for oxygen is given by:

$$G(Y_{O_2,i}) = G(Y_{O_2,C}) + L_C(0.75X_C) + G(Y_{N^*,C} - Y_{NO^*,C}) \quad (26)$$

The second term on righthand side needs some explanation. It has been assumed earlier that all the NO_x entering the cooler/condenser is in the form of NO. This NO is converted to HNO_3 through several stages: (a) NO oxidation to NO_2 according to Eq. 2; (b) conversion of NO and NO_2 to N_2O_3, N_2O_4, and HNO_2 according to Eq. 3, 4, and 5; (c) absorption of NO_2, N_2O_3, and HNO_2 to form HNO_3 and HNO_2; (d) decomposition of HNO_2 and desorption of NO. The desorbed NO need to be oxidized again. Thus, the stoichiometric oxygen requirement is greater than that indicated by Eq. 2. All the above steps may be combined to give the following equation:

$$2NO + 1.5O_2 + H_2O \longrightarrow 2HNO_3$$

Thus, it can be seen that, for the formation of 1 mol of HNO_3, 0.75 mol of oxygen is needed.

Method of solution

For the estimation of gas-phase composition and quantity of condensate (at specified temperature and concentration of condensate), we need to solve Eqs. 7-14 and 19-26. Using substitutions in Eqs. 7, 19, 24, 25, and 26 a system of five nonlinear algebraic equations having five unknowns namely Y_T, Y_{NO_2}, Y_{O_2}, L_C, and Y_{H_2O} was formulated. Under most practical conditions these five variables possess large positive value. The Newton-Raphson method in conjunction with the Gauss-Jordan method was employed. The objective behind reducing these equations was to achieve single finite solution with minimum numerical iterations.

Model for oxidizer

The gases leaving the condenser are in equilibrium with the condensate concentration. In order to produce the product acid of desired concentration it is necessary to further oxidize the nitric oxide. This is achieved by providing additional volume between the condenser and the absorber. The extent of oxidation required depends on many factors such as the desired nitric acid concentration, temperature, and pressure. The oxidation volume is usually provided at the bottom of the absorption column. Here essentially an increase in the mole fraction of tetravalent oxides occurs. Temperature in this section is maintained in the range similar to the absorption temperature of the product acid. For modeling the oxidation section, we make following assumptions: (1) gas-phase flows in the plug flow manner; (2) the oxidizer is operating at the steady state; (3) gases follow ideal gas behavior.

Gas-phase reactions and equilibria

The gas-phase reactions and equilibria have been described in the previous section. The set of Eqs. 7-16 is a mathematical formulation for establishing composition of the gas phase. Suchak et al. (1991) have reduced these eight equations to four equations expressed in Y_{NO}, Y_T, Y_{H_2O}, and Y_{NO_2}.

For a known molar concentration of inerts, oxygen, total NO_x, and NO^* to N^* ratio, equilibrium partial pressures in the gas phase can be estimated.

Model for the oxidizer section

Mass balance across a differential height dh at height h from the bottom is given as:

(a) Divalent nitrogen balance:

$$\frac{dY_{NO}^*}{dh} = -\frac{S}{G}(k_1 (p_{NO})^2 p_{O_2} \epsilon_G) \quad (27)$$

(b) Oxygen balance:

$$\frac{dY_{O_2}}{dh} = -\frac{S}{2G}\left(k_1 (p_{NO})^2 p_{O_2} \varepsilon_G\right) \tag{28}$$

Equations 27 and 28 are nonlinear differential equations. The overall oxygen and NO* balance (across the oxidizer) is established on solving these equations.

Heat balance

Oxidation of NO, formation of N_2O_3, N_2O_4, HNO_2, and HNO_3 in the gas phase are exothermic. Because of these reactions significant heat changes occur. The values of reaction rate constant and equilibrium constants depend upon temperature. Heat liberated because of various reactions in the gas phase has been included in Table 2b.

If Q_T is the total heat change per unit time in the differential element then the temperature change under adiabatic conditions is given by:

$$T_e = (Q_T + m_i^o Cp_i^o T_i)/m_e^o Cp_e^o \tag{29}$$

where T_e and T_i are the temperature at the exit and the inlet of differential element.

(a) Contribution to the heat changes from the gas phase are due to the following steps:

• The rate of formation of N_2O_3 from NO and NO_2 in the differential element is given by:

$$(N_2O_3)_f = (N_2O_3)_e - (N_2O_3)_i \tag{30}$$

$$(N_2O_3)_f = G(Y_{N_2O_3,e} - Y_{N_2O_3,i}) \tag{31}$$

The rate of heat generation due to N_2O_3 formation is:

$$Q_1 = ((N_2O_3)_f)\Delta H_4 \tag{32}$$

• The rate of formation of N_2O_4 from NO_2 in the differential element is given by:

$$(N_2O_4)_f = (N_2O_4)_e - (N_2O_4)_i \tag{33}$$

$$(N_2O_4)_f = G(Y_{N_2O_4,e} - Y_{N_2O_4,i}) \tag{34}$$

The rate of heat generation due to N_2O_4 formation is:

$$Q_2 = ((N_2O_4)_f)\Delta H_3 \tag{35}$$

• The rate of formation of HNO_3 in the differential element is given by:

$$(HNO_3)_f = (HNO_3)_e - (HNO_3)_i \tag{36}$$

$$= G(Y_{HNO_3,e} - Y_{HNO_3,i}) \tag{37}$$

The rate of heat generation due to HNO_3 formation is:

$$Q_3 = (HNO_3)_f \Delta H_6 \tag{38}$$

• The rate of formation of HNO_2 in the differential element is given by:

$$(HNO_2)_f = (HNO_2)_e - (HNO_2)_i \tag{39}$$

$$= G(Y_{HNO_2,e} - Y_{HNO_2,i}) \tag{40}$$

The rate of heat liberated due to HNO_2 formation is:

$$Q_4 = (HNO_2)_f \Delta H_7 \tag{41}$$

• The rate of heat generation due to the oxidation of NO is estimated from the knowledge of the rate of NO oxidation. It may be noted that NO is consumed in the N_2O_3 and HNO_2 formation and liberated during HNO_3 formation.

The mass balance for NO across the differential element is given by:

$$NO_o = (NO_i - NO_e) - N_2O_{3,f} - 1/2HNO_{2,f} + 1/2HNO_{3,f} \tag{42}$$

$$= G(Y_{NO,i} - Y_{NO,e} - Y_{N_2O_3,e} + Y_{N_2O_3,i} - 1/2Y_{HNO_2,e} + 1/2Y_{HNO_2,i} + 1/2Y_{HNO_3,e} - 1/2Y_{HNO_3,i}) \tag{43}$$

The rate of heat generation due to NO oxidation is given by:

$$Q_5 = (NO_{,o})\Delta H_1 \tag{44}$$

Total heat change in the differential volume is summation of all the heat changes:

$$Q_T = Q_1 + Q_2 + Q_3 + Q_4 + Q_5 \tag{45}$$

Method of solution

Estimation of Gas-Phase Composition. Solution procedure described by Suchak et al. (1991) has been used.

Solution of Ordinary Differential Equations. The solution of Eqs. 27 and 28 is a boundary value problem. The flow rate and composition of the gas phase entering the oxidizer are known. The equations were solved simultaneously by the fourth-order Runge-Kutta method. Integration was carried out until the exit of the oxidizer.

Solution of Heat Balance Equations. From the above two steps the concentrations of all species are known at the inlet and exit of the differential height. Assuming all the heat is utilized as sensible heat, temperature of the gas at the exit of the differential height is estimated. For this purpose Eqs. 29–45 were used. The effect of step size for integration was examined and it was selected in such a way that the oxidizer volume is independent of the step size.

Model for the absorption column

The absorption column employed for the manufacturing nitric acid is a plate or a packed column. The configuration is shown in Figure 1a. The cool gas stream (NO_x) is introduced at the bottom of the column in the first empty section. NO in the gas phase irreversibly oxidizes to form NO_2 affecting the equilibrium concentrations of all the other constituents of NO_x. In the case of a packed column, the empty section is followed

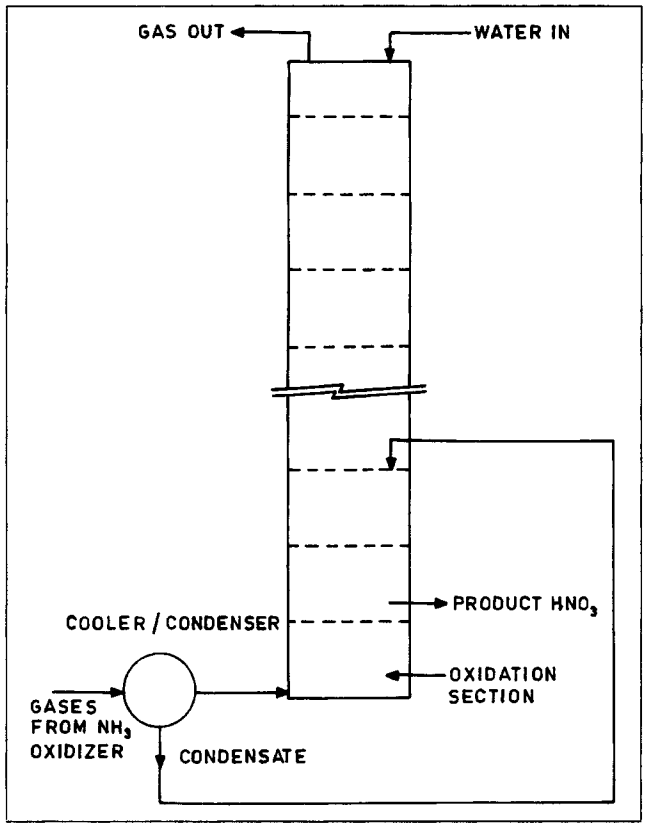

Figure 1a. NO_x absorption system for the manufacture of nitric acid.

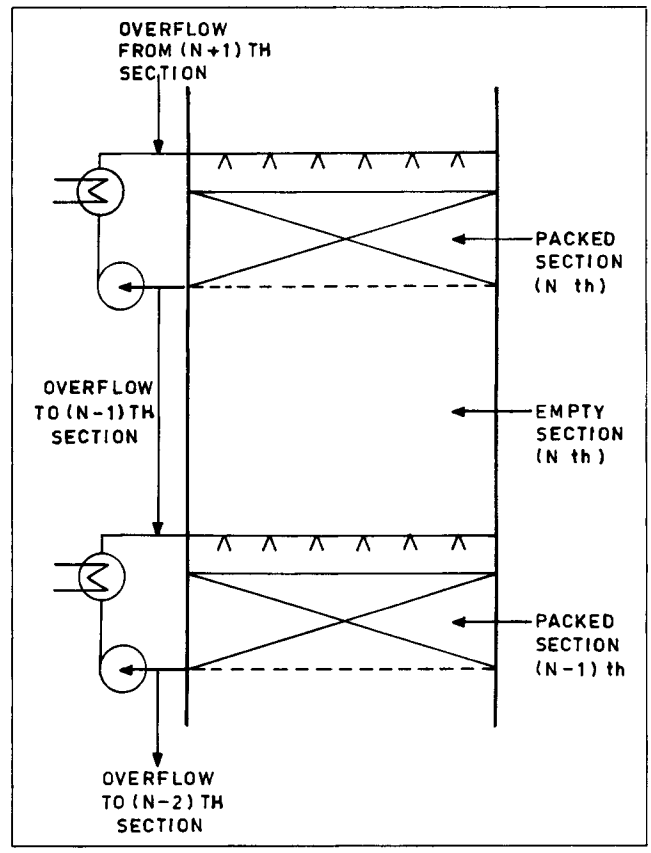

Figure 1b. One oxidation-absorption section in a packed column.

by a packed section, which is further followed by an empty section and a packed section until desired removal of NO_x is achieved. Usually one set of empty and packed sections are housed in one column. In order to ensure complete wetting of the packings, a recirculation of loop is set up as shown in Figure 1b. A heat exchanger is provided in the external loop to remove the heat of reaction. In the case of plate columns, heat-transfer coils are placed in the pool of liquid over the plate. Two plates are separated by an empty section as shown in Figure 1c. A material balance is given by the following equations.

(1) Reacted nitrogen balance over the entire column:

$$G(Y_{N^*,i} - Y_{N^*,F}) = L_P X_P \tag{46}$$

where $Y_{N^*,F}$ is mole ratio of reacted nitrogen to inerts at the column outlet.

(2) Water and water vapor balance over the entire column:

$$G(Y_{H_2O^*,i} - Y_{H_2O^*,F}) = L_P(1 + X_P/2) - F_W \tag{47}$$

$Y_{H_2O^*,F}$ is a molar ratio of saturated water vapor to inert gas at the outlet.

(3) Oxygen balance over the entire column:

$$G(Y_{O_2,i} - Y_{O_2^*,F}) = 0.75 L_P X_P + 0.5G(Y_{N^*,F} - Y_{NO^*,F}) \tag{48}$$

For the explanation of first term on the righthand side, kindly refer to the text below Eq. 26.

Model for empty section/space between plates

Model for empty section or the space between two consecutive plates is identical to that of an oxidizer already described in detail in the section discussing the model for oxidizer.

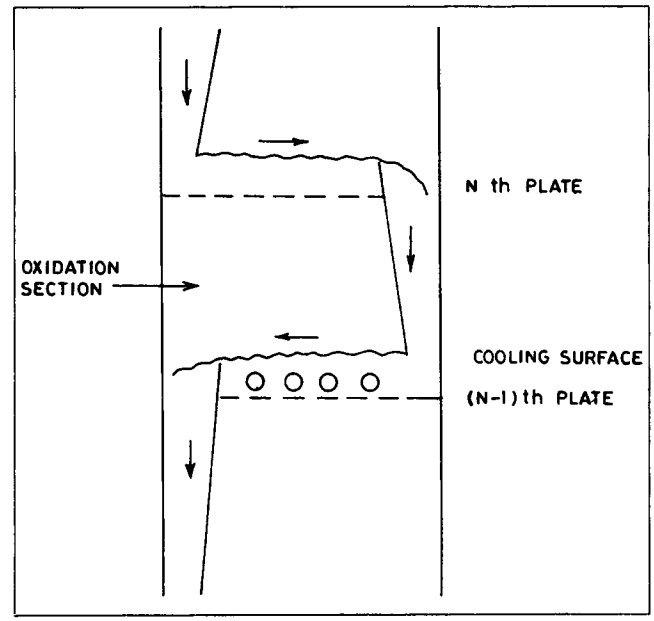

Figure 1c. One oxidation-absorption section in a plate column.

Model for absorption stage and material balance over an absorption stage

The following equations establish material balance over an absorption stage.

(1) Reacted nitrogen balance:

$$G(Y_N^{*}{}_{,N-1} - Y_N^{*}{}_{,N}) = L_N X_N - L_{N+1} X_{N+1} - L_S X_S \quad (49)$$

For the stage where the condensate (from cooler/condenser) is introduced $L_S = L_C$ and $X_S = X_C$, otherwise, $L_S = 0$.

(2) Water and Water vapor balance:

$$G(Y_{H_2O}^{*}{}_{,N-1} - Y_{H_2O}^{*}{}_{,N}) = L_N(1 + X_N/2) - L_{N+1}(1 + X_{N+1}/2) + L_S(1 + X_S/2) \quad (50)$$

Model for a packed section

A detailed model of the packed column has been presented by Suchak et al. (1991). The same model was used in the present work where the correlation for K_H values suggested by Holma and Sohlo (1979) was used. A schematic representation of one set of packed/empty sections is shown in Figure 1b.

Model for sieve plate

The liquid phase on a plate was assumed to be completely backmixed. For mass-transfer coefficients, holdup, and gas-liquid interfacial area on a sieve plate, the following correlations suggested by Zuiderweg (1982) were used:

Gas side mass-transfer coefficient:

$$k_G = 0.13/\rho_G - 0.065/\rho_G^2 \quad (51)$$

Liquid side mass-transfer coefficient:

$$k_L = 2.6 \times 10^{-5}/\eta_L^{0.25} \quad (52)$$

Gas-liquid interfacial area:

$$\underline{a} = 43/F^{0.3}(V_G^2 \rho_G h_l FP/\sigma)^{0.53}/H_W \quad (53)$$

$$\epsilon_L = 0.6 H_W^{0.5} p_H^{0.25} b^{-0.25} (FP)^{0.25}/H_W \quad (54a)$$

where:

$$FP = L'/V'(\rho_G/\rho_L)^{0.5} \quad (54b)$$

$$h_l = \epsilon_L H_W \quad (54c)$$

The absorption section model of Suchak et al. (1991) was used with design parameters of sieve plate obtained from the equations given above.

Method of solution

Computations of absorption column begins with the bottom most absorption stage. The gas-phase composition of the stream entering this absorption stage is known from the oxidizer calculations. Concentration and flow rate of product acid withdrawn are also considered to be known. From the detailed model of an absorption stage, concentrations of water vapor and reacted nitrogen in the exit stream is obtained. Concentration and the flow rate of liquid overflow from the subsequent absorption stage are the two remaining unknowns. For this purpose Eqs. 49–50 were solved by substituting Eq. 49 in 50. These calculations were repeated for all the absorption stages until the condition ($Y_N^{*} < Y_N^{*}{}_{,F}$) was satisfied. Heat balance was also established for each differential volume according to the procedure described earlier. The differential height for integration was 0.01 m for packed column and 0.002 m for plate column. There was no effect of step size below these values. Therefore, each differential volume can be considered to be isothermal. As a result, energy and species equations can be treated separately.

Results and Discussions

Simulation of a commercial plate column

Suchak et al. (1991) have shown a good agreement between model predictions and experimental observations for the case of multiple packed columns in series. It was thought desirable to simulate a sieve plate column manufacturing 750 ton/d (100% basis) of nitric acid having 58.5% concentration. This step was considered necessary before undertaking the optimization exercise. The design and operating parameters of the column are summarized in Tables 3a and 3b, respectively. The liquid submergence on each sieve plate was 50 mm. The dry pressure drop was calculated using the procedure of Fair (1984). Comparison between the predicted and the experimental concentration profiles of nitric acid are shown in Figure 2. It can be seen that the agreement is very good. The predicted outlet NO_x concentration was 1,210 ppm whereas the concentration in the commercially operating plants was 1,260 ppm. This agreement can be considered to be excellent.

Table 3a. Design Parameters of Commercial Plate Column Producing 750 tons/d Nitric Acid

Column diameter = 5.5 m
Number of plates = 73
Plate spacing = 700 mm
Liquid submergence = 50 mm
Percent free area = 3.6%
Hole diameter = 4 mm

Table 3b. Operating Parameters of Commercial Plate Column Producing 750 tons/d Nitric Acid*

(1) Total gas flow rate before the cooler-condenser = 1.69 kmol/s
(2) Total NO_x flow rate before the cooler-condenser = 0.1392 kmol/s
(3) Oxygen flow rate before the cooler-condenser = 0.1356 kmol/s
(4) Condensate temperature = 48°C
(5) Condensate concentration = 42% (w/w)
(6) Oxidizer volume = 49.9 m^3
(7) Oxidizer temperature = 38°C
(8) Inlet HNO_3 concentration = 0%
(9) Outlet HNO_3 concentration = 58% (w/w)
(10) Total pressure at the inlet of column = 0.46 MPa

*Capacity is on the basis of 100% concentration.

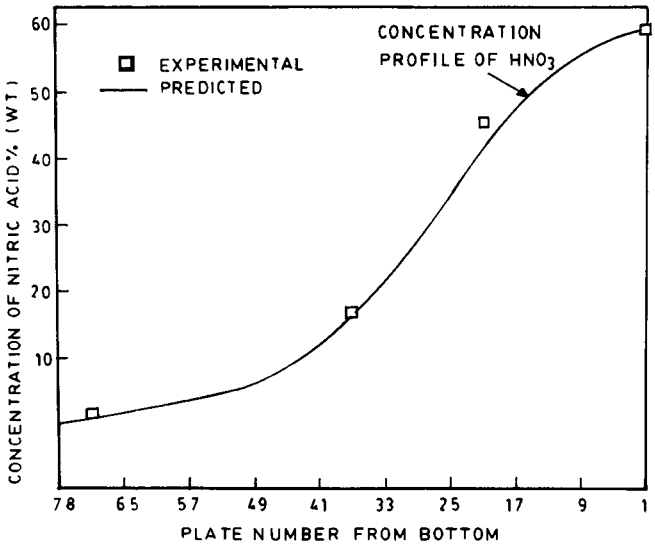

Figure 2. Simulation of a commercial nitric acid tower producing 750 ton/d.

For the design and operating parameters, refer to Table 3a.

Optimum design

(1) It has been pointed out earlier that heterogeneous equilibrium prevails between the liquid phase and the gas phase. As a result of this, for a given NO_x composition, there is a maximum permissible concentration of HNO_3 which can be produced. The concentration of HNO_3 increases with an increase in the mole fraction of tetravalent nitrogen oxides in the gas phase. Therefore, the gas phase entering the absorption column must possess sufficiently high mole fraction of tetravalent nitrogen oxides so that the absorption can occur. This condition of gas-phase composition is achieved in the oxidizer as shown in Figure 1a. Obviously, the oxidizer volume increases with an increase in the desired concentration of nitric acid.

(2) The effect of oxidation temperature on the oxidizer volume is shown in Figure 3. At any given nitric acid concentration, the oxidation volume increases with an increase in temperature. The extent of increase is very high in the temperature range of 30–45°C.

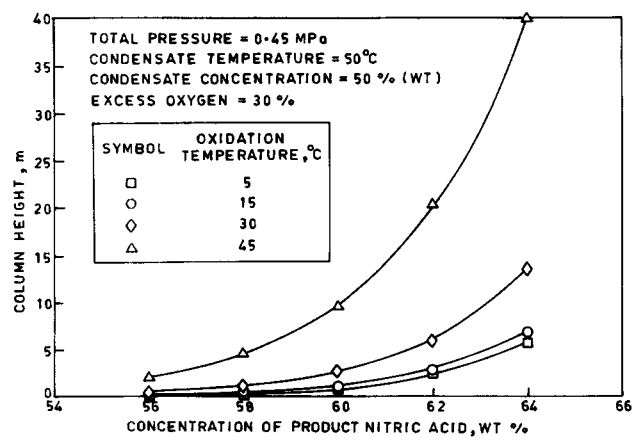

Figure 3. Effect of oxidation temperature and product nitric acid concentration on oxidizer volume.

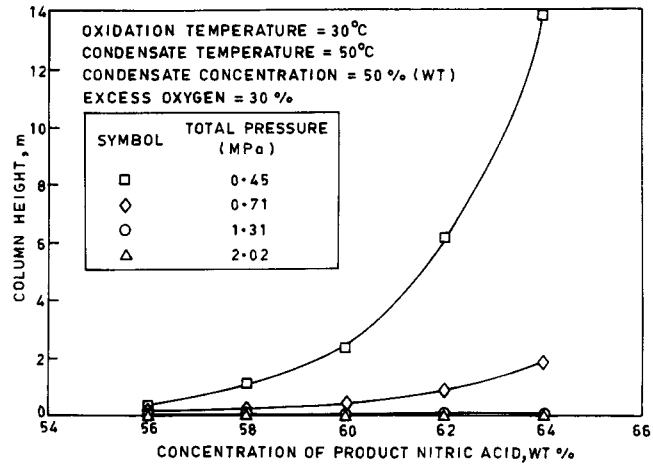

Figure 4. Effect of total pressure and product nitric acid concentration on oxidizer volume.

(3) The effect of pressure on oxidation volume is shown in Figure 4. The oxidation volume is nominal at 1.32 and 2.03 MPa. The volume increases with a decrease in pressure. The extent of increase is substantial when the pressure is reduced from 0.71 to 0.45 MPa.

(4) The effect of excess oxygen is shown in Figure 5. When the percentage excess is in the range of 10–30%, the oxidation volume decreases marginally. However, a further increase in the excess oxygen results into an increase in the oxidation volume. Such a behavior occurs because of two opposing factors. With an increase in excess oxygen, the residence time decreases due to an increase in the oxygen partial pressure. However excess oxygen is accompanied by an increase in the oxidation volume due to increase in volumetric flow rate. From Figure 5 it can be seen that 30% excess is an optimum number as far as the oxidizer volume (before the absorber) is concerned.

(5) Effects of condenser temperature and condensate concentrations are shown in Figures 6a and 6b. It can be seen from Figure 6a that the oxidation volume is negligible when the desired HNO_3 concentration is less than 60% and the condensate temperature is greater than 60°C. However, at the high temperatures of 60° and 70°C, the oxidation volume

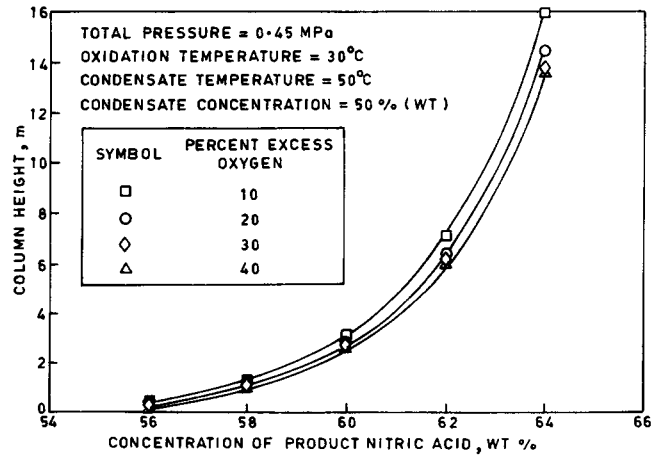

Figure 5. Effect of excess oxygen and product nitric acid concentration on oxidizer volume.

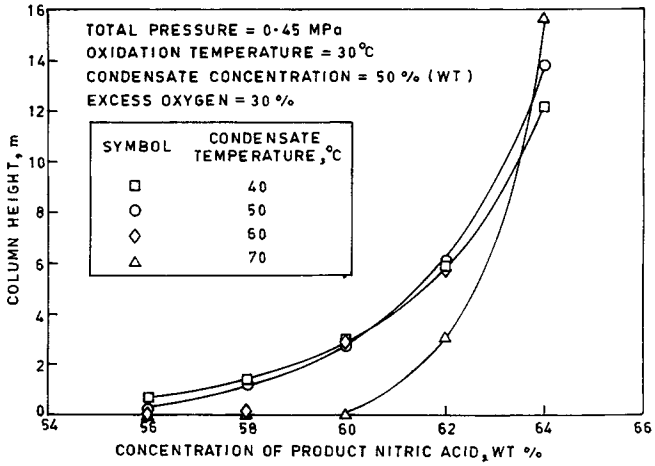

Figure 6a. Effect of condensate temperature and product nitric acid concentration on oxidizer volume.

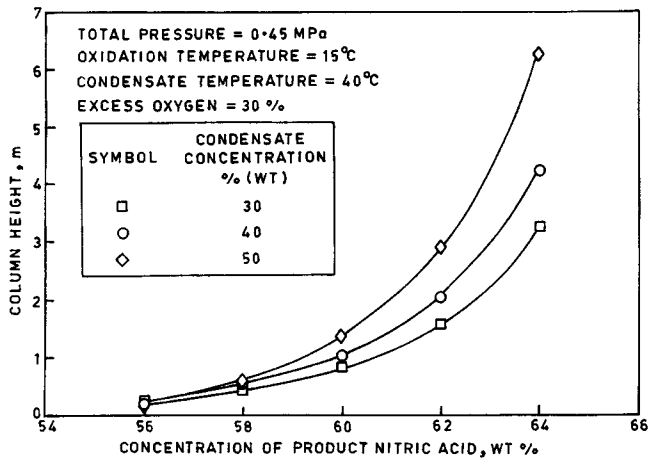

Figure 6b. Effect of condensate concentration and product nitric acid concentration on oxidizer volume.

increases sharply when the desired HNO_3 concentration increases.

When the condensate temperature is less than 50°C, the oxidation volume smoothly increases with an increase in HNO_3 concentration. It may be noted, however, that all the lines cross each other and there is a possibility of selecting an optimum oxidation volume by selecting proper condensate temperature.

From Figure 6b it can be seen that the oxidation volume increases with an increase in the condensate concentration and desired HNO_3 concentration.

In order to get an overall view regarding the number of stages needed with respect to the extent of absorption, the parameters such as pressure, temperature, and heights of packed and empty sections were varied over a wide range. The model results are given in Figures 7, 8, and 9. The capacity of absorber was 750 ton/d and 30% excess oxygen was used. Values of other parameters are listed in Table 4. From Figures 7, 8, and 9, it can be seen that the required number of stages

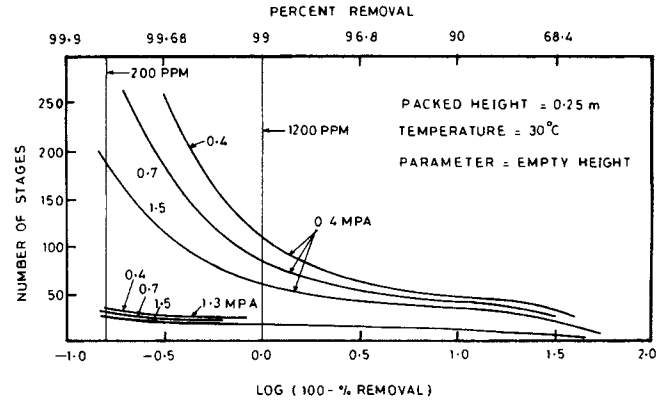

Figure 7. Effect of extent of absorption on the number of stages with pressure and height of empty section as parameters.

increases rapidly with an increase in the extent of absorption. In order to emphasize this point, the extent of conversion is shown on the top axis. Also shown are the two lines when the NO_x composition in the gas phase becomes 1,200 and 200 ppm.

The effect of total pressure and the height of empty section on the number of stages is shown in Figures 10a to 10c for packed heights of 0.25, 1.0, and 3.0 m, respectively. In all the cases, the number of stages decreases with an increase in pressure. The decrease is dramatic in the pressure range of 0.4 to 0.71 MPa. This is because the rate of oxidation varies as the cube of the pressure. However, a similar reduction is not observed when the pressure is increased from 0.71 to 1.31 MPa and further to 2.02 MPa. This is because the overall absorption becomes increasingly controlled by equilibria and the rate of oxidation is not important. This is a useful result. The oxidation volume is needed for getting sufficient tetravalent oxides so that the positive driving force prevails in the subsequent section. Such a desired composition is achieved in a small oxidation volume. In fact, at high pressures the number of stages were found to be independent of the oxidation volume (in the range covered).

From Figures 10a to 10c it can be seen that, at total pressure of 0.4 and 0.71 MPa, the number of stages decreases with an increase in the oxidation volume. Though, the number of stages

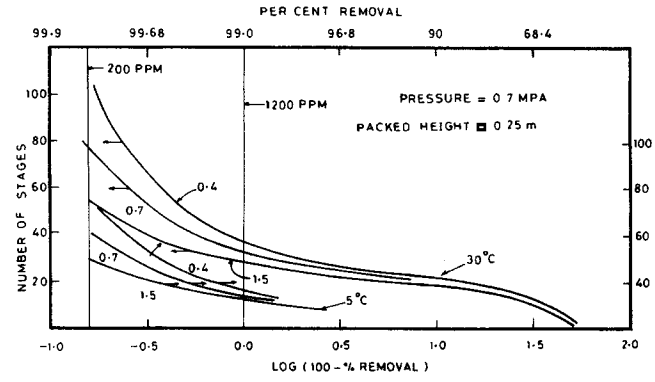

Figure 8. Effect of extent of absorption on the number of stages with temperature and height of empty space as parameter.

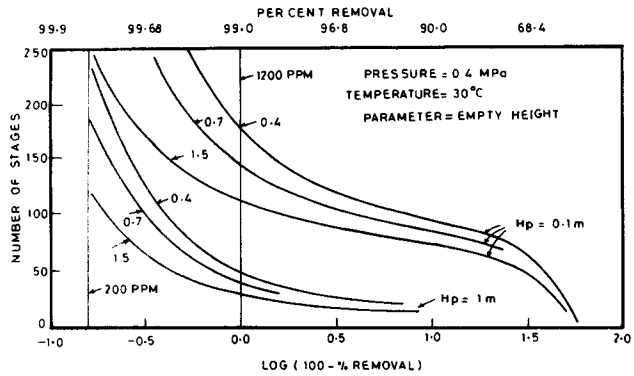

Figure 9. Effect of extent of absorption on the number of stages with the height of packed and empty sections as parameters.

decreases, it does not necessarily mean that the total height decreases. In fact, in almost all the cases, the total height was found to increase with an increase in the height of empty section (Table 5a). The increase is nominal when the empty height is increased from 0.4 to 0.7 m. This result is useful because the cost associated with a large number of stages can be reduced. However, a similar result is not obtained when the empty height is increased to 4 m and 10 m. The total height substantially increases at these empty heights. From these results it can be seen that there is an optimum level of NO oxidation per stage. A very high level of conversion needs more oxidation volume and it is not useful since some NO is liberated in the subsequent absorption section. An empty height of 0.7 m looks favorable.

The effect of packed height is shown in Figure 11 and Table 5b. It can be seen that the effect of packed height is not as dramatic as the empty height. The optimum packed height lies in the range of 0.25 to 0.5 m. The effect of temperature on the number of stages and total height is shown in Figure 12 and in Table 5c. In this case also the optimum empty height can be considered as 0.7 m and the optimum packed height is in the range of 0.25 to 0.5 m.

Though the total height is substantially low at lower temperatures, it may not be economically advantageous to operate the absorption column at low temperatures due to high refrigeration costs. However, the liquid ammonia feedstock pro-

Table 4. Values of Parameters

Values of Parameters for Figures 3 to 12	
Capacity	= 750 ton/d
Total gas-flow rate before cooler condenser	= 1.69 kmol/s
Total NO_x flow rate before cooler condenser	= 0.1352 kmol/s
Oxygen flow rate before cooler condenser	= 0.1356 kmol/s
Superficial liquid velocity	= 5 mm/s
Column diameter	= 5.5 m
Packing	= Intalox saddles
Packing size	= 37 mm
Packing voidage	= 0.77
Additional Parameters for Figures 7 to 12	
Condensate temperature	= 50°C
Condensate concentration	= 50% (wt.)
Concentration of product nitric acid	= 58% (wt.)
Additional Parameter for Figures 10 to 12	
Outlet NO_x	= 700 ppm

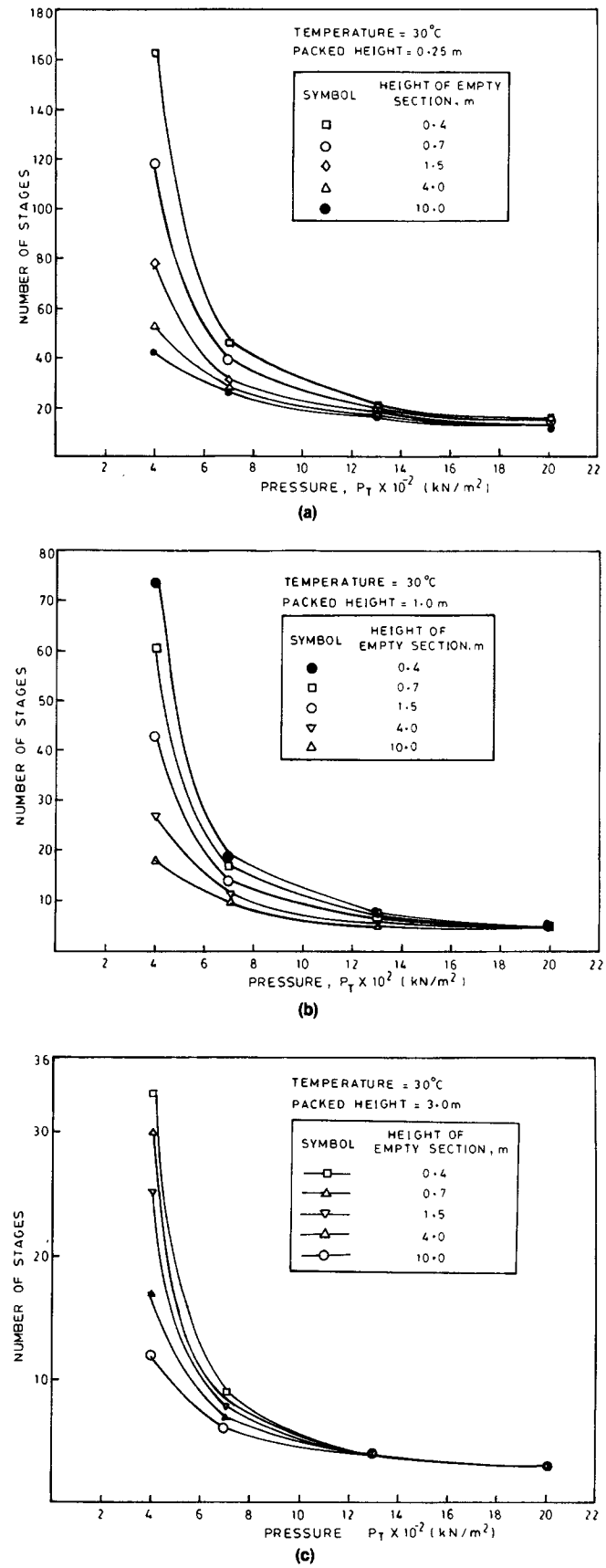

Figure 10. Effect of total pressure and the height of empty section on number of stages.

Packed height: A = 0.25 m; B = 1.0 m; C = 3.0 m.

Table 5a. Total Column Height*

Height of Empty Section H_E, m	Packed Height H_P, m	Total Column Height, m, Pressure, MPa 0.4	0.71	1.31	2.02
0.4	0.25	105.95	29.90	13.65	10.40
0.7	0.25	112.10	37.05	19.00	14.25
1.5	0.25	138.25	56.00	33.25	26.25
4.0	0.25	225.25	119.00	72.25	63.75
10.0	0.25	430.25	266.50	184.50	143.50
0.4	1.00	103.60	26.60	11.20	7.00
0.7	1.00	103.60	28.90	13.60	8.50
1.5	1.00	107.50	35.00	17.50	12.50
4.0	1.00	135.00	55.00	35.00	25.00
10.0	1.00	198.00	110.00	66.00	55.00
0.4	3.00	112.20	30.60	13.60	10.20
0.7	3.00	111.00	29.60	14.80	11.10
1.5	3.00	112.50	36.00	18.00	13.50
4.0	3.00	119.00	49.00	28.00	21.00
10.0	3.00	156.00	78.00	52.00	39.00

*Parameters are listed in Table 4; temperature = 30°C.

Table 5b. Total Column Height*

Height of Empty Section H_E, m	Packed Height H_P, m	Total Column Height, m, Pressure, MPa 0.4	0.71	1.31	2.02
0.7	0.10	128.00	62.40	38.40	30.40
0.7	0.25	90.25	36.10	13.65	16.15
0.7	0.50	79.20	27.60	14.40	10.80
0.7	1.00	76.20	25.50	11.90	10.20
0.7	3.00	81.40	25.90	14.80	11.10

*Parameters are listed in Table 4; temperature = 15°C.

Table 5c. Total Column Height*

Height of Empty Section H_E, m	Packed Height H_P, m	Total Column Height, m, Temperature, °C 5	15	30	40
0.4	0.25	72.15	79.95	105.95	131.95
0.7	0.25	84.55	90.25	112.10	140.60
1.5	0.25	120.75	120.75	138.25	168.00
0.7	0.10	130.40	128.00	144.80	172.80
0.7	0.50	72.00	79.20	103.20	133.20
0.7	1.00	68.00	76.50	103.70	134.30

*Parameters are listed in Table 4; pressure = 0.4 MPa.

vides for some refrigeration load. The rate of heat removal due to vaporization of liquid ammonia can be used advantageously in the top section where the rate of oxidation is very low. Most of the heat is usually removed by the ambient water. Hence, the operating temperature is decided by the ambient temperature. Some refrigeration may, however, be used after establishing a clear economic advantage.

From Figures 10a to 10c and Table 5a it can be seen that the total height substantially decreases with an increase in the total pressure. The equipment cost will decrease with an increase in pressure. This is because the reduction in volume and an increase in wall thickness with pressure results into an overall decrease in the metal requirement. However, this should be traded off with operating expenses for compression (after giving due credit to the energy recovery in the turbine).

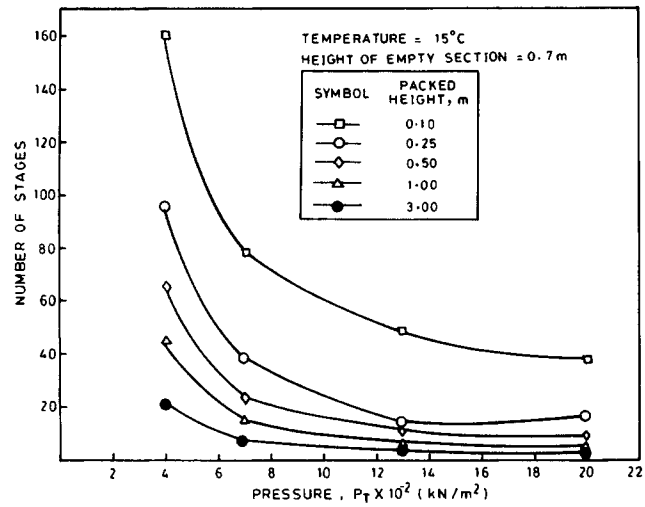

Figure 11. Effect of total pressure and the packed height on number of stages.

From the foregoing discussion it can be seen that the optimum heights for empty section and packed section can be selected directly. However, the optimum temperature and pressure depend upon the geographical location and the cost of power.

The results on packed columns are presented in Figures 7 to 12 and Table 5 and are for the design and operating parameters listed in Table 4. For a plate column (% free area, hole diameter, and column diameter are given in Table 3a), a similar exercise resulted into the following correlations:

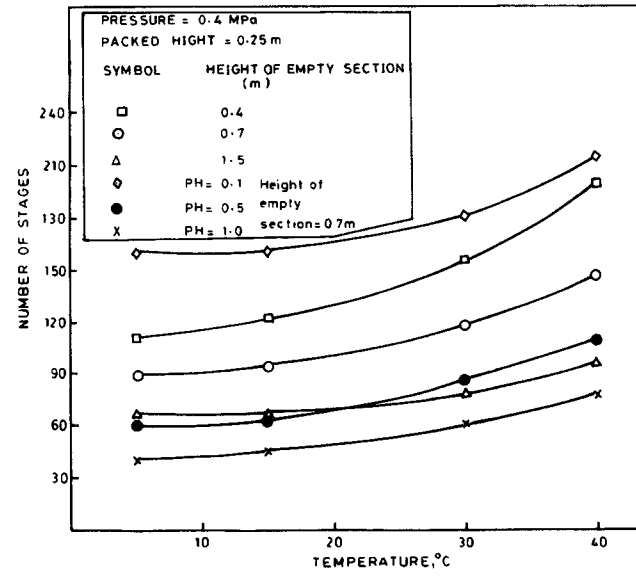

Figure 12. Effect of temperature and the height of empty section and the packed height on the number of stages.

$$0.2 < H_E < 1.5 \text{ m}$$

$$N = 482.74 H_E^{-0.434} H_W^{-0.144} \exp(-1{,}221.6/P_T) \times \exp(-1{,}563.1/T) \quad (55a)$$

$$1.5 < H_E < 10 \text{ m}$$

$$N = 28.01 H_E^{-0.177} H_W^{-0.199} \exp(658.8/P_T) \exp(-555.7/T) \quad (55b)$$

where

$$0.4 < H_E < 10 \text{ m}, \quad 0.025 < H_W < 0.1 \text{ m},$$

$$0.4 < P_T < 2.02 \text{ MPa and } 278 < T < 318 \text{ K}$$

Conclusions

(1) A mathematical model has been developed for the prediction of optimum design of packed and plate columns. The effects of inlet NO_x composition, temperature, pressure, volume of pre-oxidizer, volume of interstage oxidizers, and extent of absorption per stage have been included in the model.

(2) The concentration of product nitric acid strongly depends upon the inlet NO_x composition, temperature, pressure, and excess oxygen. For a given concentration of product nitric acid, the optimum design of preoxidizer has been presented.

(3) The extent of oxidation per stage strongly influences the number of stages. The overall equipment volume was found to increase with an increase in the extent of oxidation. However, the number of stages increases with a decrease in the extent of oxidation.

(4) The optimum design depends nominally on the extent of absorption per stage.

(5) Correlations have been developed for the number of stages for plate and packed absorption columns.

Notation

a = interfacial area, m^2/m^3
b = weir length per unit bubbling area, m^{-1}
C_P^o = average specific heat of liquid phase, kcal/kmol$^1 \cdot K^1$
D = diffusivity, m^2/s
F = fraction of hole area per unit bubbling area
FP = flow parameter, $L'/V' \sqrt{\rho_G/\rho_L}$
F_W = feed water, kmol/s
G = flow rate of inerts, kmol/s
h = height from bottom of the spray column, m
h_l = volume of liquid per unit plate area, m^2/m^3
H = total height of the column, m
H_e = Henry's low coefficient, kmol/m^2 (kN/m^2)
H_E = height of empty section, m
H_p = height of packed section, m
H_W = weir height, m
k = reaction rate constant, s^{-1}
k_1 = forward reaction rate constant for Eq. 1
k_G = gas-side mass-transfer coefficient, kmol/[$m^2 \cdot$s(kN/m^2)]
k_L = liquid-side mass-transfer coefficient, m/s
k_n = forward reaction rate constant for reaction n
K_6 = heterogeneous equilibrium constant defined by Eqs. 21 and 23, $(kN/m^2)^{-0.5}$
K_H = heterogeneous equilibrium constant, Eqs. 22a and 22b, atm^{-2}
K_n = equilibrium rate constant for reaction n
L = molar flow rate of liquid, kmol/s
L' = mass-flow rate of liquid, kg/s
L_P = flow rate of water in the product acid, kmol/s
m^o = mass-flow rate of liquid, kmol/s
N^* = total moles of NO_x
NO^* = total moles of divalent nitrogen oxides
p_H = pitch of holes, m
p_n = partial pressure of component n, kN/m^2
P_T = total pressure of gas, kN/m^2
Q_1 = heat changes due to formation of N_2O_3 in bulk gas, kcal/s
Q_2 = heat changes due to formation of N_2O_4 in bulk gas, kcal/s
Q_3 = heat changes due to formation of HNO_3 in bulk gas, kcal/s
Q_4 = heat changes due to formation of HNO_2 in bulk gas, kcal/s
Q_5 = heat changes due to formation of NO in bulk gas, kcal/s
Q_T = total heat changes, kcal/s
S = cross-sectional area of the column, m^2
T = temperature, K
V' = mass-flow rate of gas, kg/s
V_G = superficial gas velocity, m/s
W = weight fraction of HNO_3 in aqueous nitric acid solution
X = moles of nitric acid per mole of water
$Y_{H_2O}^*$ = kmol of water in form of oxyacids and free water in gas phase per kmol of inerts
Y_N^* = kmol of reactive nitrogen per kmol of inerts
$Y_{N^*,F}$ = moles of reaction nitrogen per mole of inerts in the gas stream leaving absorber
$Y_{N^*,i}$ = moles of reacted nitrogen per mole of inerts in the gas stream from NH_3 oxidizer
Y_{NO}^* = kmol of divalent nitrogen per kmol of inerts
$Y_{NO^*,F}$ = moles of divalent nitrogen oxides per mole of inerts in the gas stream leaving absorber
$Y_{O_2}^*$ = moles of oxygen per mole of inerts
$Y_{O_2,F}$ = moles of oxygen per mole of inerts in the gas stream leaving absorber
$Y_{O_2^*,i}$ = moles of oxygen per mole of inerts in the gas stream from NH_3 oxidizer
Y_T = total moles of gas per mole of inerts
Y_x = moles of gaseous component x per mole of inerts

Greek letters

ΔH_x = heat of reaction for reaction given by Eq. x
ϵ_G = fractional gas holdup
ϵ_L = fractional liquid holdup
η_L = kinematic viscosity of liquid, m^2/s
ρ = density, kg/m^3
σ = surface tension, N/m

Subscripts

a = absorption
C = condensate
e = exit condition
f = formation
F = outlet
G = gas phase
i = inlet condition
L = liquid phase
N = nth stage
S = side stream from condenser to column
T = total

Literature Cited

Andrew, S. P. S., and D. Hanson, "The Dynamics of Nitrous Gas Absorption," *Chem. Eng. Sci.*, **14**, 105 (1961).

Carberry, J., "Some Remarks on Chemical Equilibrium and Kinetics in the Nitrogen Dioxide-Water System," *Chem. Eng. Sci.*, **9**, 189 (1958).

Carleton, A. J., and F. H. Valentin, *Proc. Eur. Symp. Chem. Reaction Eng.*, Pergamon, Oxford, p. 361 (1968).
Counce, R. M., and J. J. Perona, "Gaseous Nitrogen Oxide Absorption in a Sieve Plate Column," *Ind. Eng. Chem. Fund.*, **18**, 400 (1979b).
Counce, R. M., and J. J. Perona, "A Mathematical Model for Nitrogen Oxide Absorption in a Sieve Plate Column," *Ind. Eng. Chem. Proc. Des. Dev.*, **19**, 426 (1980).
Counce, R. M., and J. J. Perona, "Scrubbing of Gaseous Nitrogen Oxides in Packed Towers," *AIChE J.*, **29**, 26 (1983).
Emig, G., K. Wohlfahrt, and U. Hoffmann, "Absorption with Simultaneous Complex Reactions in Both Phases, Demonstrated by the Modeling and Calculation of Counter-Current Flow Columns for the Production of Nitric Acid," *Comput. Chem. Eng.*, **3**, 143 (1979).
Fair, J. R., "Gas-Liquid Contacting" in *Chemical Engineers' Handbook*, R. H. Perry and C. H. Chilton, eds., McGraw Hill Kogakusha, Tokyo (1984).
Holma, H., and J. Schlo, "A Mathematical Model for an Absorption Tower of Nitrogen Oxides in Nitric, Acid Production," *Comput. Chem. Eng.*, **3**, 135 (1979).
Hoftizer, P. J., and F. J. G. Kwanten, "Absorption of Nitrous Gases," G. Nonhabel, *Gas Purification Processes for Air Pollution Control*, Butterworths, London (1972).
Joshi, J. B., V. V. Mahajani, and V. A. Juvekar, "Absorption of NO_x Gases," *Chem. Eng. Commun.*, **33**, 1 (1985).
Koukolik, M., and J. Marek, *Proc. 4th Eur. Symp. Chem. React. Eng.*, Pergamon, Oxford, p. 347 (1968).
Koval, E. J., and M. S. Peters, "Reaction of Aqueous Nitrogen Dioxide," *Ind. Eng. Chem.*, **52**, 1011 (1960).
Makhotkin, A. F., and A. M. Shamsutdinov, *Khim. Khim. Tekhnol.*, **19**(9), 1411 (1976).
Miller, D. N., "Mass Transfer in Nitric Acid Absorption," *AIChE J.*, **33**, 1351 (1987).
Sherwood, T. K., R. L. Pigford, and C. R. Wilke, *Mass Transfer*, McGraw-Hill, New York (1975).
Suchak, N. J., K. R. Jethani, and J. B. Joshi, "Computer Aided Design of NO_x Gases in Water, Nitric Acid and Mixed Solution of Nitric and Sulphuric Acids," *AIChE J.*, **36**, 323 (1991).
Wiegand, K. H., E. Scheibler, and M. Thiemann, "Computations for Plate Columns for NO_x Absorption by a Stage to Stage Method," *Chem. Eng. Technol.*, **13**, 289 (1990).
Zuiderweg, F. J., "Sieve Trays," *Chem. Eng. Sci.*, **37**, 1441 (1982).

Errata

◆ In the article titled "Memory-Integral Mass-Transfer Models for Adsorption Process Simulation" (March 1993, p. 422) by G. M. Harriott, the following corrections are made:

• On p. 425, fifth full paragraph, the last sentence should read: "Galerkin projection forces the error to be orthogonal to the basis function. . ."

• On p. 426, Table 2, the solution for Galerkin Projection: Linear Basis should contain a term of $\pi/3$, not $\pi/6$ as reported.

• On p. 428, the coefficients $\{a, b\}$ in the formulae for harmonic forcing (Eq. 28) should be multiplied by 2. The phase lag is $\phi = \tan^{-1}(b/a)$, and the asymptotic form of the amplitude A at large frequency ω is: $A \rightarrow 3/\sqrt{\omega}$.

• On p. 432, sentences 6 and 7 of the first paragraph should read: "On desorption, however, the pellet does not unload until concentration drops below $1/H$, and since the driving force for diffusion is then $O(1/H)$, a time of $O(H)$ is required to clean out the pellet. The ratio of timescales for desorption to adsorption is simply the isotherm slope at low concentration: H."

• The title of the article by Glueckauf (1955) is "Theory of Chromatography: 10. Formulae for Diffusion Into Spheres and Their Application to Chromatography."

◆ Correct affiliations of the authors of the article titled "Two Methods of Selecting Smoothing Splines Applied to Fermentation Process Data," (April 1994, p. 716) are as follows:

Nina F. Thornhill
Dept. of Electronic and Electrical Engineering

Mauro Manela and John A. Campbell
Dept. of Computer Science

Karl M. Stone
Advanced Centre for Biochemical Engineering,
University College London, Gower Street, London WC1E 6BT